

Coalescence of Sessile Polymer Droplets: A Molecular Dynamics Study

Soheil Arbabi Panagiotis E. Theodorakis*

S. Arbabi, P. E. Theodorakis

Institute of Physics, Polish Academy of Sciences, Al. Lotników 32/46, 02-668 Warsaw, Poland

Email Address: panos@ifpan.edu.pl

Keywords: *Droplet Coalescence, Polymer Chains, Droplet Dynamics, Molecular Dynamics Simulation*

Droplet coalescence is ubiquitous in nature and the same time key to various technologies, such as inkjet printing. Here, we report on the coalescence of polymer droplets with different chain lengths coalescing on substrates of different wettability. By means of molecular dynamics simulations of a coarse-grained model, it is found that the rate of bridge growth is higher in the case of droplets with smaller contact angles (more wettable substrates) and decreases with the increase of the chain length of the polymers. Different behavior has also been identified in the dynamics of the approach of the two droplets during coalescence with the substrate wettability playing a more important role compared to the chain length of the polymers. While the dynamics of the droplet are greatly affected by the latter parameters, the density profile and flow patterns remain the same for the different cases. Thus, we anticipate that our work provides further insights into the coalescence of liquid polymer droplets on solid substrates with implications for relevant technologies.

1 Introduction

Droplet coalescence is ubiquitous in nature and at the same time much relevant for various technologies, such as spraying and printing [1, 2], where the rate of this process can determine the efficiency of the application. The primary factor controlling coalescence is the interplay of viscous and inertial forces as droplets minimise their total surface-tension energy by coalescing [3]. Despite research in this area [4–10], droplet coalescence remains a fascinating phenomenon with many of its aspects calling for further investigations to reach adequate understanding of this phenomenon in various scenarios [4–10]. On the one hand, part of this gap in knowledge is due to device limitations, since experiments cannot capture the initial fast stages of droplet coalescence. On the other hand, the singularity at the contact point during the initial stages of coalescence presents challenges for numerical modelling [8, 10, 11], despite progress in this area [10], while hydrodynamic models are only applicable at the later stages of coalescence [12–14]. Apart from device and methodology limitations, further understanding at molecular scales is much desirable as applications often require greater control at nanoscales. Moreover, the role of a substrate in the coalescence of sessile droplets deserves further consideration despite research in this area by theory and experiment [15–19], especially in the context of complex liquids containing various additives, such as polymers and colloids.

Droplet coalescence takes place in three stages, with the first being the initial droplet approach when the droplets are close enough to interact with each other and form in between the so-called bridge. Then, the bridge-growth stage follows, which eventually results in the final reshaping of the two droplets towards the equilibrium state of a single spherical-cap droplet, which is the state of minimum energy. From the perspective of fluid dynamics the initial bridge growth is generally driven by viscous forces, as a result of the interactions between molecules, while inertial forces dominate the coalescence process at the later stage [8, 11]. In the case of the viscous regime, a linear scaling in time $b \propto t$ has been suggested for the bridge radius, b , or logarithmic corrections $t \ln t$, while a scaling $b \propto \sqrt{t}$ has been proposed for the inertial regime [8]. However, the dynamics of the bridge growth is still under debate, for example, an inertially limited viscous regime has been reported [20, 21] or the proposition of a modified Ohnesorge number in the case of immiscible droplets for coupling the linear and power-law scalings [22]. All-atom molecular dynamics (MD) simulations [7] have described the initial stage of the bridge growth for water droplets, not achievable by continuum simulation or experiment. In particular, the formation of multiple precursor bridges at the pinch point were observed, which result from thermal capillary waves that exist at the droplets' surface. In this case, simulations suggest that multiple bridges that expand linearly in time develop at the surface and the transition to the classical hydrodynamics regime only takes place

when the bridge radius exceeds a thermal length defined as $l_T \approx (k_B T / \gamma)^{1/4} R^{1/2}$, where k_B is Boltzmann's constant, T the temperature, γ the liquid–vapour (LV) surface tension, and R the radius of the droplets.

In the case of droplet coalescence on solid substrates, much less is known, despite the immediate implications for applications, for example, in coatings [23] and microfluidics [24] technologies. In particular, in the case of coalescence of low-viscosity droplets on a substrate it has been experimentally found that the bridge height, b , grows with time as $t^{2/3}$ when the contact angle is below 90° , while a scaling $b \propto t^{1/2}$ has been observed for contact angles above 90° [16], which is the scaling found in the inertial regime for freely suspended drops [8, 23]. Moreover, a geometrical model that unifies the inertial coalescence of sessile and freely suspended drops and can capture the transition from the $2/3$ to the $1/2$ exponent in the case of sessile droplets has been proposed [16]. In addition, in the case of asymmetric coalescence, that is droplets with different contact angles, the theory predicts that the shape of the bridge can be described by similarity solutions of the one-dimensional lubrication theory, with the bridge growing linearly in time and exhibiting dependence on the contact angles [15]. In earlier experimental studies, a power-law growth at early times as $t^{1/2}$ has been suggested for the symmetric case, while the growth rate appeared to be sensitive to both the radius and the height of the droplet with a scaling H/R , where H is the height of the droplet from the substrate to its apex and R its radius [23]. Further experimental work on droplets with contact angles in the range 10° – 56° has found that the bridge growth scales as a power law with exponents in the range 0.5061 to 0.8612 with data deviating from the power law at longer times during coalescence for contact angles larger than 24° . Moreover, a power law with an exponent 0.2901 has been found for the width of the bridge [17]. Finally, further experimental work has focused on analysing the morphology and dynamics of droplet coalescence on substrates [25].

Despite previous work on the coalescence of sessile droplets, many aspects of this phenomenon require further investigation. One of them is the role of viscosity in the coalescence for substrates with different wettability. Viscosity is expected to play a role, especially in the context of polymer droplets studied here, where in addition to surface-tension-effects differences, entanglement effects may also play a role for longer polymer chains or the polymer–polymer interactions close to the contact line in both the initial and later stages of coalescence. Here, we attempt to elucidate these points and fill in the gap in knowledge in this area by carrying out molecular dynamics simulations of a coarse-grained model for droplets comprised of polymer chains with different length on substrates of different wettability with equilibrium contact angles of individual droplets above and below 90° . We find that the bridge length dynamics are much slower in the case of polymer droplets than what is observed for water droplets. Moreover, the coalescence process considerably slows down with the increase of polymers chain length. Furthermore, more wettable substrates have consistently faster bridge growth dynamics in comparison with the less wettable substrates. The wettability of the substrate also affects significantly the dynamics of the bridge angle and the approach of the coalescing droplets, while the viscosity of the droplets appears to have a smaller effect. In the following, we describe our simulation model and method. Then, we discuss our results, while in the final section we draw our conclusions.

2 Simulation model and methods

Our system consists of two polymer droplets placed next to each other as shown in **Figure 1** to initiate their coalescence. Each droplet contains polymer chains with the same number of monomers (beads), N . The polymer chains are modelled by the standard bead–spring model [26–28], where all beads interact with a truncated and shifted Lennard-Jones (LJ) potential,

$$U_{\text{LJ}}(r) = 4\varepsilon_{\text{ij}} \left[\left(\frac{\sigma_{\text{ij}}}{r} \right)^{12} - \left(\frac{\sigma_{\text{ij}}}{r} \right)^6 \right]. \quad (1)$$

This interaction is applied for beads within the cutoff distance $r_c = 2.5 \sigma$, where σ is the length unit. The interaction between polymer beads is $\varepsilon_{\text{pp}} = \epsilon$, where ϵ is the unit of energy. The temperature of the system is, $T = \epsilon/k_B$, where k_B is Boltzmann's constant. Moreover, consecutive beads along a polymer

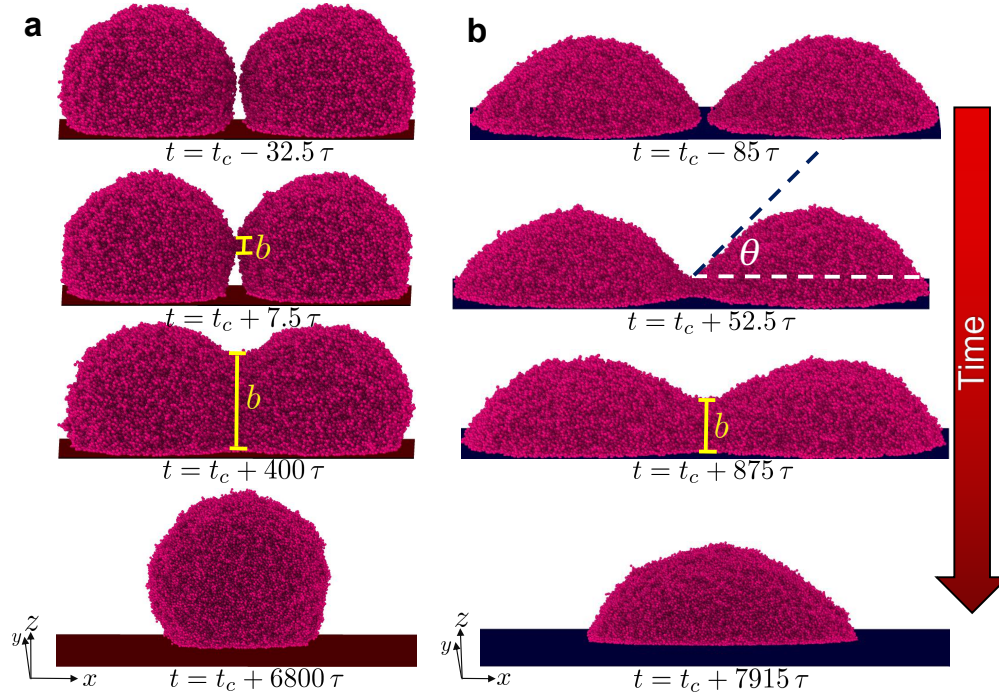


Figure 1: Evolution of the droplet coalescence on a solid substrate with a lower (a, $\epsilon_{pw} = 1.1 \epsilon$) and a higher (b, $\epsilon_{pw} = 2.5 \epsilon$) wettability as a function of time, t , from the first permanent contact of the droplets at time t_c , as indicated. Here, $N = 10$ beads. Moreover, the angle, θ , and the bridge length, b , are indicated. The implicit, smooth substrate modelled by the 9–3 LJ potential of Equation 3 is illustrated by a solid colour.

chain are tethered by the “finitely extensible nonlinear elastic” (FENE) potential,

$$U_{\text{FENE}}(r) = -0.5K_{\text{FENE}}R_0^2 \ln \left[1 - \left(\frac{r}{R_0} \right)^2 \right], \quad (2)$$

where r is the distance between two consecutive beads along the polymer chain, $R_0 = 1.5 \sigma$ expresses the maximum extension of the bond, and $K_{\text{FENE}} = 30 \epsilon / \sigma^2$ is an elastic constant. The length of the polymer chain in this model in effect varies the viscosity of the droplets [29]. Here, the chain length is the same for both droplets in each system and is chosen in the range $N = 10 - 640$ beads. Since the total number of beads in each droplet is 57600, using longer chains would also require the increase of the overall size of the droplet, in order to ensure that the majority of the chains are not on the surface of the droplet, thus avoiding artifacts that may not apply in macroscopic droplets. Moreover, increasing N and the total number of beads in the droplets would result in longer times required for the equilibration of the initial droplets and the coalescence experiments to reach the final equilibrium stage. Still, it would be valuable to extend the range of N in future investigations and carry out a full scaling analysis of droplet properties on the chain length N and the overall droplet size. The wettability of the substrate by the droplet is controlled through the parameter ϵ_{pw} of the 9–3 LJ potential, which describes the interaction of the polymer beads with an implicit, smooth wall [30],

$$U_w(z) = 4\epsilon_{pw} \left[\left(\frac{\sigma_s}{z} \right)^9 - \left(\frac{\sigma_s}{z} \right)^3 \right], \quad (3)$$

where z is the normal (vertical) distance of the beads from the substrate within a cutoff distance $z_c = 2.5 \sigma$. Here, $\sigma_s = \sigma$.

To evolve our system in time and control the temperature of the system, the Langevin thermostat is used as done previously [31]. The equation of motion for the coordinates $\{r_i(t)\}$ of the beads of mass m (m is the unit of mass)

$$m \frac{d^2 \mathbf{r}_i}{dt^2} = -\nabla U_i - \gamma \frac{d\mathbf{r}_i}{dt} + \Gamma_i(t). \quad (4)$$

is numerically integrated for each bead using the LAMMPS package [32]. In Equation 4, t denotes the time, U_i is the total potential acting on the i th bead, γ is the friction coefficient, and $\Gamma_i(t)$ is the random force. As is well-known, γ and Γ are related by the usual fluctuation–dissipation relation

$$\langle \Gamma_i(t) \cdot \Gamma_j(t') \rangle = 6k_B T \gamma \delta_{ij} \delta(t - t'). \quad (5)$$

Following previous work [31, 33, 34], the friction coefficient was chosen as $\gamma = 0.5 \tau^{-1}$. Equation 4 was integrated using an integration time step of $\Delta t = 0.01 \tau$, where the time unit is $\tau = (m\sigma^2/\epsilon)^{1/2}$. A single droplet is first equilibrated for adequate time, so that the total energy has reached a minimum and properties, such as the mean contact angle and average shape of the droplet do not change with time. Then, the equilibrated droplet is cloned and positioned on the substrate as shown in Figure 1. In this case, the size of the box is chosen such to accommodate the two droplets avoiding the interaction of mirror images of the droplets due to the presence of periodic boundary conditions in all Cartesian directions. Moreover, the use of polymer droplets leads to the absence of vapour in the system [35], which greatly facilitates the analysis of the trajectories and maintaining the same thermodynamic conditions during the simulation of either the individual droplet or the two coalescing droplets. Different scenarios of substrate wettability were considered in our study, for which ϵ_{pw} is 2.5ϵ or 1.1ϵ . In this case, the equilibrium contact angles of the individual droplets before coalescence are 78° and 118° , respectively. To estimate the contact angle of the droplet, a method that avoids a fitting procedure is used, which has been described in Reference [36]. We have also found that the equilibrium contact angles of the individual droplets do not show any statistically significant dependence on the length, N , of the polymer chains.

To analyse the bridge growth dynamics, snapshots of the system are frequently dumped, especially for the initial stage, typically every 250 integration time steps and beads are assigned to a three-dimensional grid with size 2.5σ in all directions. For the analysis of each snapshot, the center of the bridge is located in the middle of the grid, corresponding to the position $x = 0$ in the x direction of the coordinate system and any rotation of the droplets around the z axis has been removed. This facilitates our analysis and guarantees that our measurements of the bridge radius and all other properties (*e.g.* density profiles) remain consistent as coalescence proceeds. The snapshots of Figure 1 have been taken after performing the above procedure, which is manifested by the perfect alignment of the droplets along their long axis in the x direction and the bridge is also placed in the middle of the substrate on the $x - y$ plane. The three dimensional grid is also used to calculate the profile of the number density of the droplets by considering a slab along the $x - z$ plane in the x direction that passes through the center of the bridge. Further details regarding the calculation of the various properties are provided later during the discussion of the respective results.

3 Results and Discussion

Figure 1 shows typical coalescence cases on substrates with different wettability, corresponding to contact angles of lower and greater than 90° . A key parameter for characterising the dynamics of the coalescence process is the bridge length, b , which is indicated for each case in Figure 1. When the substrate is less wettable (contact angle greater than 90°), the bridge initially forms above the substrate at the contact point between the LV interface of the coalescing droplets, and later comes into contact with the substrate as the coalescence process proceeds (Figure 1a). In contrast, in the case of more wettable substrates (contact angles lower than 90°), the bridge grows onto the substrate from the beginning of the coalescence process. While the time that bridge is in contact with the substrate is expected to affect the dynamics of the droplets, in the case of more wettable substrates the interaction between the droplet and the substrate is also stronger.

Figure 2 presents our results for the dynamics of the bridge length, b , on the two different substrates. Apart from the initial thermal regime [7], we find that in terms of the bridge length the dynamics of coalescence on both substrates can be described by a power-law behaviour ($\sim t^\beta$) with exponents that are clearly lower than $1/2$ (contact angles greater than 90°) and $2/3$ (contact angles lower than 90°), which

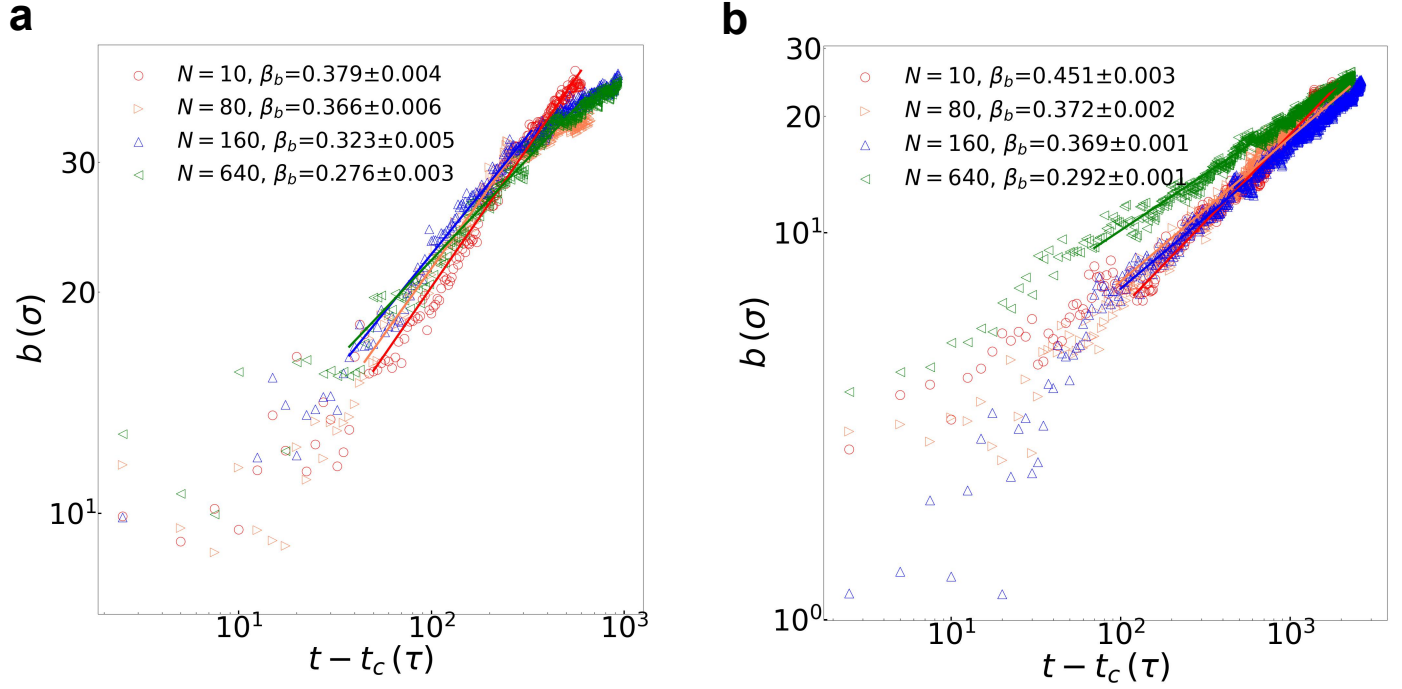


Figure 2: Bridge length, b , as a function of time, t , counting from the time of first permanent contact of the coalescing droplets, t_c . Data for polymer droplets with different chain length are shown, N , as indicated. (a) $\varepsilon_{pw} = 1.1 \epsilon$; (b) $\varepsilon_{pw} = 2.5 \epsilon$. The power-law exponents ($\sim t^{\beta_b}$) are reported for the bridge length with values of $\chi^2/\text{ndf} \approx 1$, where ndf indicates the number of degrees of freedom.

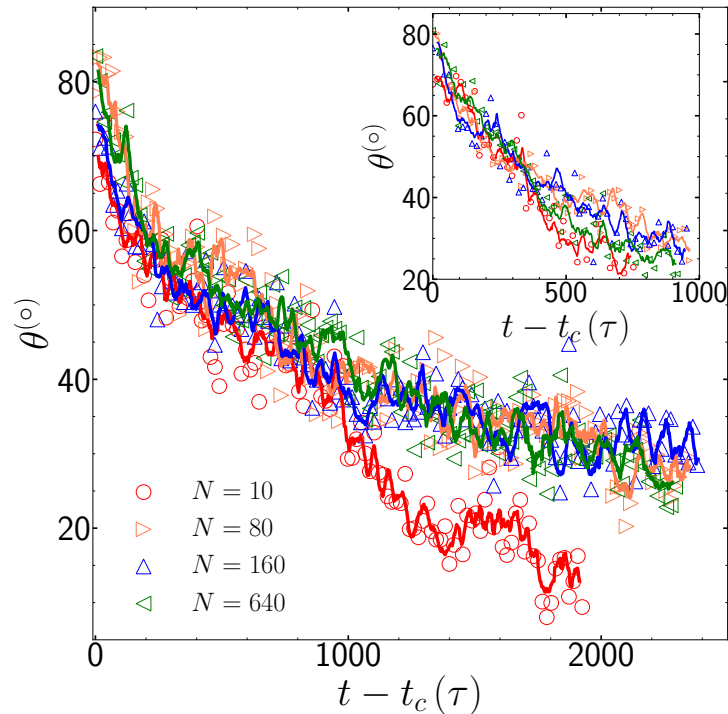


Figure 3: Angle θ (see Figure 1 and main text for further details) as a function of time, t , counting from the time of first permanent contact of the coalescing droplets, t_c . Data for polymer droplets with different chain length, N , are shown, as indicated. The lines are a guide for the eye. Here, $\varepsilon_{pw} = 2.5 \epsilon$ and $\varepsilon_{pw} = 1.1 \epsilon$ (inset).

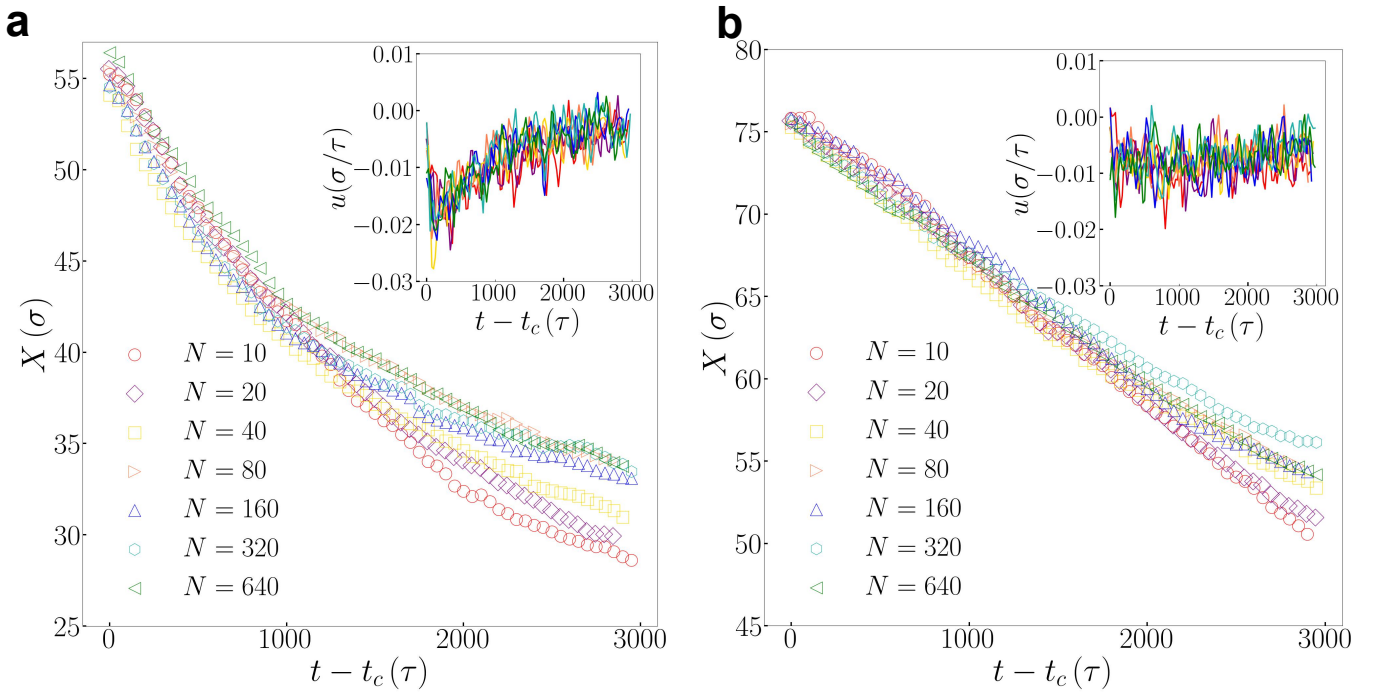


Figure 4: Distance X in the x direction between the centre of mass of coalescing droplets for cases of different chain length, N , as indicated. Insets show the instantaneous velocity of approach $u = dX/dt$. (a) $\varepsilon_{pw} = 1.1 \epsilon$; (b) $\varepsilon_{pw} = 2.5 \epsilon$.

have been reported for water droplets [16]. Therefore, our results suggest that the rate of coalescence is slower in the case of polymer droplets compared to the case of water droplets. Moreover, the increase of the polymer chain length leads to gradually decreasing values of the power-law exponent for both types of substrates. However, exponents are clearly higher in the case of the more wettable substrate, which suggests that the coalescence process be faster when the attraction of the polymer chains to the substrate is stronger. Hence, an increased substrate wettability appears to accelerate the dynamics of the bridge growth, thus facilitating droplet coalescence throughout the range of N studied here. Moreover, we have identified the presence of a second regime at the final stages of the coalescence process and when almost the bridge has been fully developed in the case of less wettable substrates, an effect that is more pronounced for longer chain lengths N . In summary, we find that an increasing chain length of the droplets will slow down the coalescence of polymer droplets and more wettable substrates will exhibit faster dynamics than less wettable substrates with power-law exponents, β_b , significantly lower than what has been observed for sessile water droplets.

Figure 3 presents results for the angle θ at the bridge (see Figure 1). A symmetric angle is defined for the second droplet of Figure 1 and the average of the two angles for each snapshot is considered as the value of the angle θ . To calculate the angle θ , one considers a horizontal plane that passes through the top of the bridge. Then, the angle is calculated based on the curvature of the droplets as discussed in a previous study, thus avoiding a fitting procedure [36]. Estimating the angles can in general be highly sensitive to the details of the definition of a sharp interface, as well as the fitting procedure [37,38]. Moreover, models that could account for the disjoining pressure effects, for example, in the context of droplets on solid substrates, might perform better than fitting spherical caps to nanodroplets [37]. In general, our data for the angle θ appear noisier than the data referring to the bridge length. One of the main reasons for this are the larger fluctuations on the droplets shape during the coalescence process. Hence, a discussion here can only focus on the dynamics of the angle θ , which seems to be greater affected at the earlier times of coalescence in the case of more wettable substrates, while curves seem to saturate for chain lengths $N \geq 80$ beads. Moreover, a faster rate of change appears in the case of the less wettable substrates.

We have further explored the dynamics of the coalescence process by monitoring the distance X of the

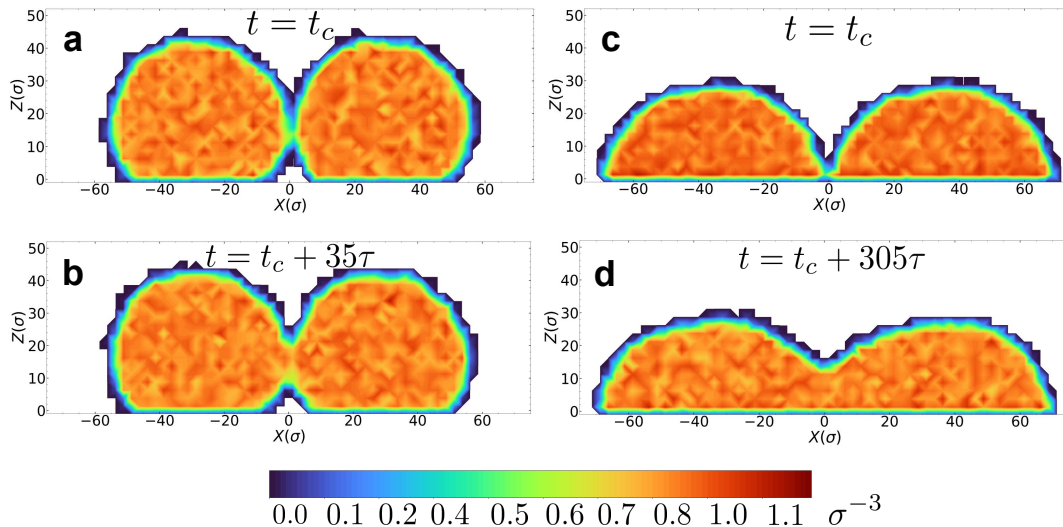


Figure 5: Profiles of the number density along a cross-section in the x direction ($x - z$ plane) of the coalescing droplets ($N = 640$ beads) at different stages (upper panels correspond to snapshots obtained at time t_c , when the droplets come into permanent contact). (a, b) $\varepsilon_{pw} = 1.1 \epsilon$; (c, d) $\varepsilon_{pw} = 2.5 \epsilon$.

centre of mass of the coalescing droplets, and, also, calculated its derivative with time, which reflects the instantaneous velocity of approach of the droplets (**Figure 4**). Our data for $\varepsilon_{pw} = 1.1 \epsilon$ (less wettable substrate) show two different dynamics regimes with a transition between them that is more pronounced in the case of droplets with longer polymer chains ($N \geq 40$ beads). This transition seems to become smoother as the chain length decreases. Moreover, the instantaneous velocity, u , of the approach of the droplets is higher at the initial stages of coalescence and then rather reaches a smaller value, which remains constant until the bridge has fully developed. This velocity appears to be similar for the different systems, independently of the chain length. In the case of the systems with $\varepsilon_{pw} = 2.5 \epsilon$, a different behaviour is observed. X steadily decreases, while the velocity, u , obtains small values over the entire coalescing process with the initial instantaneous velocity of the approach of the droplets to exhibit a slightly higher (more negative velocity, since the distance X decreases) velocity. Hence, although the bridge growth dynamics is faster in the case of the more wettable substrate, the approach of the two droplets appears slower in the case of the more wettable substrate.

Finally, we have calculated the density profiles of the droplets during coalescence. From the obtained results, we have not identified any noticeable changes in the density profiles for droplets of different chain length and substrates with different wettability. We have also analysed the flow patterns and they have also not revealed any noticeable differences for the different systems. Typical density profiles for various cases are presented in **Figure 5** at an initial stage of the coalescence process, when droplets come into contact, and at a later stage when the bridge has been clearly developed. Hence, while the dynamics of the coalescence process depends on the choice of the substrate and the chain length of the polymers, no noticeable changes in the patterns of the density and the flow are observed during coalescence for the various cases considered in our study.

4 Conclusions

In this study, we have characterised the dynamics of the coalescence of polymer droplets with different chain lengths on substrates with different wettability, where the contact angle of individual droplets is less and above 90° . The rate of coalescence is a key property and can be characterised by the growth rate of the bridge length. We find that polymer droplets overall show a slower rate of the bridge growth in comparison with what has been observed in the case of water droplets in experiments. Moreover, the

dynamics are slower as the length of the polymer chains of the droplets increases. Also, we find that more wettable substrates will exhibit faster dynamics, which suggests that a stronger attraction between the droplet and the substrate will accelerate the bridge growth. In addition, we have characterised the dynamics of the approach of the two droplets based on the distance between the centre of masses of the coalescing droplets. The behaviour is different when the wettability of the substrate changes with two different regimes being more pronounced in the case of less wettable substrates. In this case, differences in the dynamics between droplets with different chain lengths have been also observed. While the dynamics of the coalescence can vary when the length of the polymer chains or the substrate wettability vary, the density and velocity profile patterns do not reveal any dependence on these parameters. Thus, we anticipate that our study provides insights in the coalescence of liquid polymer droplets on solid substrates.

Acknowledgements

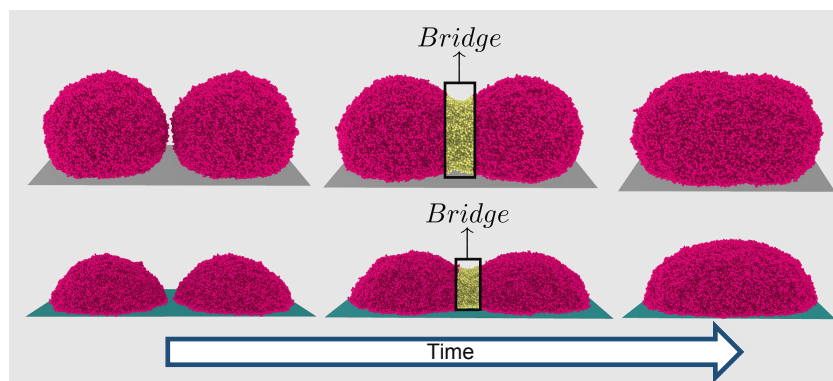
This research has been supported by the National Science Centre, Poland, under grant No. 2019/34/E/ST3/00232. We gratefully acknowledge Polish high-performance computing infrastructure PLGrid (HPC Centers: ACK Cyfronet AGH) for providing computer facilities and support within computational grant no. PLG/2022/015261.

References

- [1] J. Eggers, E. Villermaux, *Rep. Prog. Phys.* **2008**, *71*, 3 036601.
- [2] H. Wijshoff, *Phys. Rep.* **2010**, *491*, 4 77.
- [3] C. Verdier, M. Brizard, *Rheol. Acta* **2002**, *41* 514.
- [4] J. D. Paulsen, R. Carmigniani, A. Kannan, J. C. Burton, S. R. Nagel, *Nat. Commun.* **2014**, *5* 3182.
- [5] Y. Yoon, F. Baldessari, H. D. Ceniceros, L. G. Leal, *Phys. Fluids* **2007**, *19*, 10 102102.
- [6] M. I. Khodabocus, M. Sellier, V. Nock, *Adv. Math. Phys.* **2018**, *2018*.
- [7] S. Perumanath, M. K. Borg, M. V. Chubynsky, J. E. Sprittles, J. M. Reese, *Phys. Rev. Lett.* **2019**, *122*, 10 104501.
- [8] J. Eggers, J. R. Lister, H. A. Stone, *J. Fluid Mech.* **1999**, *401* 293.
- [9] D. G. Aarts, H. N. Lekkerkerker, H. Guo, G. H. Wegdam, D. Bonn, *Phys. Rev. Lett.* **2005**, *95*, 16 164503.
- [10] J. E. Sprittles, Shikhmurzaev, *Phys. Fluids* **2012**, *24* 122105.
- [11] L. Duchemin, J. Eggers, C. Josserand, *J. Fluid Mech.* **2003**, *487* 167.
- [12] L. Y. Yeo, O. K. Matar, E. S. P. de Ortiz, G. F. Hewitt, *J. Colloid Interface Sci.* **2003**, *257*, 1 93.
- [13] Y. Hu, D. Pine, L. G. Leal, *Phys. Fluids* **2000**, *12*, 3 484.
- [14] A. Mansouri, H. Arabnejad, R. Mohan, In *Fluids Engineering Division Summer Meeting*, volume 46216. American Society of Mechanical Engineers, **2014** V01AT05A006.
- [15] J. F. Hernández-Sánchez, L. A. Lubbers, A. Eddi, J. H. Snoeijer, *Phys. Rev. Lett.* **2012**, *109* 184502.
- [16] A. Eddi, K. G. Winkels, J. H. Snoeijer, *Phys. Rev. Lett.* **2013**, *111* 144502.
- [17] M. W. Lee, D. K. Kang, S. S. Yoon, A. L. Yarin, *Langmuir* **2012**, *28*, 8 3791.
- [18] W. D. Ristenpart, P. M. McCalla, R. V. Roy, H. A. Stone, *Phys. Rev. Lett.* **2006**, *97* 064501.

- [19] N. Kapur, P. H. Gaskell, *Phys. Rev. E* **2007**, *75* 056315.
- [20] J. D. Paulsen, J. C. Burton, S. R. Nagel, S. Appathurai, M. T. Harris, O. A. Basaran, *Proc. Natl. Acad. Sci. U.S.A.* **2012**, *109*, 18 6857.
- [21] J. D. Paulsen, *Phys. Rev. E* **2013**, *88*, 6 063010.
- [22] H. Xu, T. Wang, Z. Che, *J. Colloid Interface Sci.* **2022**, *628* 869.
- [23] W. Ristenpart, P. McCalla, R. Roy, H. Stone, *Phys. Rev. Lett.* **2006**, *97*, 6 064501.
- [24] S. Feng, L. Yi, L. Zhao-Miao, C. Ren-Tuo, W. Gui-Ren, *Chinese J. Anal. Chem.* **2015**, *43*, 12 1942.
- [25] N. Kapur, P. H. Gaskell, *Phys. Rev. E* **2007**, *75* 056315.
- [26] M. Murat, G. S. Grest, *Phys. Rev. Lett.* **1989**, *63* 1074.
- [27] P. E. Theodorakis, S. A. Egorov, A. Milchev, *J. Chem. Phys.* **2017**, *146*, 24 244705.
- [28] P. E. Theodorakis, S. A. Egorov, A. Milchev, *Europhys. Lett.* **2022**, *137*, 4 43002.
- [29] R. Kajouri, P. E. Theodorakis, P. Deuar, R. Bennacer, J. Židek, S. A. Egorov, A. Milchev, *Langmuir* **2023**, *39*, 7 2818.
- [30] P. E. Theodorakis, Y. Wang, A. Chen, B. Liu, *Materials* **2021**, *14*, 9.
- [31] P. E. Theodorakis, W. Paul, K. Binder, *Eur. Phys. J. E* **2011**, *34*, 12 52.
- [32] S. Plimpton, *J. Comp. Phys.* **1995**, *117* 1.
- [33] G. S. Grest, M. Murat, *Macromolecules* **1993**, *26*, 12 3108.
- [34] M. Murat, G. S. Grest, *Macromolecules* **1991**, *24*, 3 704.
- [35] N. Tretyakov, M. Müller, *Soft Matter* **2013**, *9* 3613.
- [36] P. E. Theodorakis, E. A. Müller, R. V. Craster, O. K. Matar, *Soft Matter* **2015**, *11*, 48 9254.
- [37] P. Yatsyshin, S. Kalliadasis, *J. Fluid Mech.* **2021**, *913* A45.
- [38] F. Mugele, T. Becker, R. Nikopoulos, M. Kohonen, S. Herminghaus, *J. Adhes. Sci. Technol.* **2002**, *16*, 7 951.

Table of Contents



Droplet coalescence of polymer droplets exhibits faster bridge growth for more wettable substrates (contact angle lower than 90°) and slower for droplets with longer polymer chains. The dynamics of droplets' approach are different for less wettable substrates (contact angle higher than 90°) with two different regimes identified as the growing bridge comes into contact with the substrate.